Unifying the dark sector through a single matter fluid with nonzero pressure

Peter K. S. Dunsby,[1,2,3,4,*] Orlando Luongo,[5,6,7,8,9,†] and Marco Muccino[5,9,‡]

[1]*Department of Mathematics and Applied Mathematics, University of Cape Town, Rondebosch 7701, Cape Town, South Africa*
[2]*Cosmology and Gravity Group (CGG), University of Cape Town, Rondebosch 7701, Cape Town, South Africa*
[3]*South African Astronomical Observatory, Observatory 7925, Cape Town, South Africa*
[4]*Centre for Space Research, North-West University, Potchefstroom 2520, South Africa*
[5]*Università di Camerino, Via Madonna delle Carceri 9, 62032 Camerino, Italy*
[6]*SUNY Polytechnic Institute, 13502 Utica, New York, USA*
[7]*Istituto Nazionale di Fisica Nucleare, Sezione di Perugia, 06123, Perugia, Italy*
[8]*INAF—Osservatorio Astronomico di Brera, 20121 Milano, Italy*
[9]*NNLOT, Al-Farabi Kazakh National University, Al-Farabi avenue 71, 050040 Almaty, Kazakhstan*

(Received 2 September 2023; accepted 13 December 2023; published 9 January 2024)

We explore a generalized unified dark energy model that incorporates a nonminimal interaction between a tachyonic fluid and an additional scalar field. Specifically, we require that the second field possesses a vacuum energy, introducing an ineliminable offset due to a symmetry-breaking mechanism. After the transition (occurring as due to the symmetry-breaking mechanism of the second field), the corresponding equation of state (EoS) takes the form of a combination between a generalized Chaplygin gas (GCG) component and a cosmological constant contribution. We reinterpret this outcome by drawing parallels to the so-called Murnaghan EoS, widely-employed in the realm of solid-state physics to characterise fluids that, under external pressure, counteract the pressure's effect. We examine the dynamic behavior of this model and highlight its key distinctions compared to the GCG model. We establish parameter bounds that clarifies the model's evolution across cosmic expansion history, showing that it, precisely, exhibits behavior akin to a logotropic fluid that eventually converges to the ΛCDM model in the early universe, while behaving as a logotropic or Chaplygin gas at intermediate and late times respectively. We explain our findings from a thermodynamic perspective, and determine the small perturbations in the linear regime. At very early times, the growth factor flattens as expected while the main departures occur at late times, where the Murnagham EoS results in a more efficient growth of perturbations. We discuss this deviation in view of current observations and conclude that our model is a suitable alternative to the standard cosmological paradigm, introducing the concept of a matterlike field with nonzero pressure.

DOI: 10.1103/PhysRevD.109.023510

I. OVERVIEW

Assuming that on large scales the geometry of the universe is described by a Robertson-Walker metric, observations have conclusively shown that the expansion of the universe is currently accelerating [1–10]. This phenomenon is commonly attributed to the thermodynamic properties of an exotic fluid with an unknown negative EoS that yields an effective repulsive gravity [11–13]. This cosmic speed up cannot be attributed to ordinary fluids, such as dustlike matter or radiation, for which the pressures are zero and one third, respectively, thus acting to decelerate the universe today.

Thus, the common belief is that there exists an additional exotic fluid which is responsible for the cosmic speed-up [12,14,15], whose nature is currently attributed to the cosmological constant, Λ [16] or, more broadly to some sort of dark energy contribution [17]. However, this scenario is absolutely not exhaustive yet and, in fact, the precise nature of this fluid remains very poorly understood [18]. Several conjectures have been put forward to explain the origins of the acceleration and identify the constituents responsible for it [19–25].

As stated above, the cosmological constant appears as the principal candidate responsible for the cosmic speed-up, making the concordance model statistically favored [26] as it depends on one parameter only, namely the cosmic mass. However, there are still conceptual and theoretical issues raised by observed cosmological tensions [27], which are yet to be solved. Nevertheless, dark energy remains a

*peter.dunsby@uct.ac.za
†orlando.luongo@unicam.it
‡marco.muccino@lnf.infn.it

plausible explanation for these issues [28]. Unfortunately, having an evolving EoS also provides nonequilibrium effects and, moreover, we do not have direct evidence for dark energy reconstruction.

Additionally, the nature of dark matter provides a further challenge for theoretical cosmology [29]. It is known to interact through gravity, but its properties beyond that, i.e., microphysics, scattering properties, structure, etc., are still not well understood [30]. Several candidates have been proposed, such as ultralight fields, extremely massive particles, geometric contributions, extensions of Einstein's gravity and so forth [29,31] albeit no direct evidence has been found so far [32]. Consequently, the search for dark matter particles is ongoing, through experiments involving direct and indirect detection. Discovering dark matter origin would represent one of the most significant breakthroughs in our understanding toward the universe and its constituents.

Even though dark energy and dark matter are often considered as separate and completely different components [33], some theories propose a unified approach in which a single dark fluid can explain both phenomena[1] [35]. Recently, unified models, also known as *unified dark energy or dark matter models*, have been proposed to eliminate the degrees of freedom due to quantum fluctuations in the early universe [36]. These models have been characterized by barotropic fluids or scalar fields [37] and the main assumption is that the fluid is a single entity, rather than a sum of dark matter and dark energy, and its net pressure is negative enough to drive the universe's present-day acceleration [38]. Indeed, unifying dark energy and dark matter has two significant advantages: first, it requires only a single component to explain both the observed accelerated expansion and structure formation; second, it enables us to treat dark matter and dark energy at the perturbation level in the same way [39]. The prototype of such models is the Chaplygin gas [40–42]. These models have however been severely criticized in the last decade [43]. On the other hand, dark fluids [44] and logotropic models [45] are also possible alternative toward unifying dark energy and dark matter, however, again, a pure logotropic model cannot describe the universe's dynamics as shown in Ref. [46], while a dark fluid needs additional explanations, as shown in Refs. [47,48].

Motivated by these ideas, we explore how to construct a single dark fluid with almost negligible pressure at early times, but negative pressure at late times. To do so, we assume a tachyonic field minimally-coupled to a further scalar field carrying vacuum energy. The underlying scenario is to incorporate vacuum energy under the form of a quantum field cosmological constant into a tachyonic field that provides similar behavior than previous unified dark energy models, such as the Chaplygin gas [41]. We obtain this way a Chaplygin-like gas that includes quantum fluctuations as due to a symmetry breaking mechanism associated with the field transporting vacuum energy. Consequently, we find that an effective dark matter field arises, reducing at late times to a genuine cosmological. Contrary to the standard ΛCDM paradigm, our model induces a net pressure at early times that influences structure formation. Hence, the coincidence problem appears to be resolved, since dark energy evolves in time, i.e., the corresponding effective framework works as a generalization of the Chaplygin gas with vacuum energy. Afterward, we search for a physical interpretation of our fluid and demonstrate that our EoS is akin to the *Murnaghan fluid* [49], where a *single matter fluid* with nonzero EoS shows dust and dark energy as the cosmological scale changes. In particular, this implies that matter is not described by a dustlike fluid, but it behaves differently on cosmic scales. The Murnaghan fluid, initially proposed in contexts of solid state physics, is therefore applied to the universe at different scales. To this end, the fluid naturally invokes the existence of a negative EoS we first physically interpret it in view of the background dynamics and then investigate how it affects the clustering of structures at early times.

Different stages are thus investigated to get constraints on the free parameters of the model, showing a good compatibility with observations. To do so, we work out the most recent type Ia supernovae (SNe Ia), baryonic acoustic oscillation (BAO) and observational Hubble data (OHD) catalogs to perform Markov chain Monte Carlo (MCMC) simulations based on Metropolis-Hastings algorithm, and compare our findings with the standard background ΛCDM model. Further, we explore the thermodynamics of the Murnaghan fluid highlighting the main differences with respect to the Chaplygin gas. Specifically, we show that there are regions in which the model predicts a logotropic behavior, emphasizing the consequences on the observable universe, while having regions in which the fluid acts as a dark fluid. In other words, we conclude that our scenario predicts a unified model that incorporates previous frameworks into a single fluid of matter with pressure, making it a serious candidate for an alternative description of dark energy on large scales.

The paper is organized as follows. In Sec. II, we describe how to incorporate vacuum energy into a tachyonic field coupling it to a further scalar minimally-coupled with the first one. In such a way, we introduce the basic demands of the Murnaghan fluid that is better described in Sec. III, emphasizing the corresponding thermodynamics of the fluid itself and the limiting cases predicted by our approach. In Sec. IV, we work out our numerical analysis. In Sec. V, in view of our numerical analysis, we propose a physical interpretation of our fluid, discussing in particular the thermodynamic consequences

[1]This idea is similar to the concept of extended and/or modified gravity scenarios [34], where an additional fluid can be inferred from the field theory.

of our recipe. Hence, introducing the concept of *matter with pressure*, we study the impact of such a scenario on linear perturbations, in Sec. VI. Finally, in Sec. VII, we present the conclusion and perspectives of our work.

II. MINIMALLY COUPLED TACHYONIC FIELD WITH VACUUM ENERGY

The existence of matter with nonzero pressure has posed a longstanding challenge in modern cosmology [50]. This concept has been extensively explored in the frameworks of *unified dark energy* models, where dark matter is characterized by a nonzero pressure. These models offer a way to unify these two elusive components of the universe, where the primary unknown ingredient becomes solely dark matter. Noteworthy, such models can be derived from fundamental representations that consider the Lagrangian of specific fields associated with the dark matter constituent. By incorporating these unified models, we can potentially gain a deeper understanding of the nature and properties of dark matter and its interplay with dark energy.

A prototype of these models is represented by the dark fluid. Here, one has *one fluid only*, determined by an EoS that resembles the total EoS induced by the ΛCDM model, where instead, at late times, two fluids are involved, i.e., dust plus the cosmological constant Λ. A possible definition of dark fluid is recovered from the *quasi-quintessence fluid* [51–53], induced by an energy-momentum tensor of the form

$$\rho = K(\partial\phi) + U(\phi), \tag{1a}$$

$$P = -U(\phi), \tag{1b}$$

where $U > 0$ is the potential induced by a scalar field, whose generalized kinetic energy $K(\partial\phi)$ is a function of the velocity $\partial\phi \equiv \partial^\mu\phi$ of the scalar field, ϕ. The Lagrangian representation can be written by means of $\mathcal{L} = K - U + \lambda Y$, with λ the Lagrange multiplier. For additional details see Ref. [48]. The quasiquintessence fluid is capable of solving the cosmological constant problem, as demonstrated in Ref. [51] and so it appears a viable alternative to the standard background model [48,54,55].

Even though quite relevant, the dark fluid is not the unique example of unified models of dark energy. Among all the other possibilities, some relevant approaches are the well-established Chaplygin gas or its generalizations [40,41,56]. These models have been extensively investigated at late and early times, providing a fundamental representation in terms of tachyonic fields [57,58]. Incidentally, tachyon condensate cosmological models have been first considered in a class of string field theories [59] and have gained further consideration in the literature [60,61].

Motivated by such considerations, an interesting extension of the above models may also consider the case in which a tachyonic fluid transports vacuum energy, in analogy to the cosmological constant. To do so, we demand that a nonminimally coupled tachyonic field incorporates vacuum energy by means of a further field transporting it.

Thus, we conjecture the existence of a Lagrangian able to feature both a GCG model and a cosmological constant and consider

$$\mathcal{L}_s = b(\phi)f(X), \tag{2}$$

where $X \equiv \partial_\sigma\phi\partial^\sigma\phi$ is the kinetic term of the field ϕ and $b(\phi)$ and $f(X)$ are analytical functions. Given the action $\hat{S} = \int \mathcal{L}_s\sqrt{-g}dx^4$, the energy-momentum tensor reads

$$T_{\mu\nu} = -\frac{2}{\sqrt{-g}}\frac{\delta\hat{S}}{\delta g^{\mu\nu}} = -2\frac{\delta\mathcal{L}}{\delta g^{\mu\nu}} + g_{\mu\nu}\mathcal{L}, \tag{3}$$

and the four-velocity $u_\mu = \partial_\mu\phi/\sqrt{X}$, the pressure and the density of this fluid become

$$\rho_s = b(\phi)f(X) - 2Xb(\phi)f_X(X), \tag{4a}$$

$$P_s = -b(\phi)f(X), \tag{4b}$$

where f_X labels the derivative of f with respect to the kinetic term.

It turns out that, in this framework, a constant term in the EoS cannot be recovered either assuming algebraic equations for $b(\phi)$ and $f(X)$, or by assuming $b = b(\phi, \nabla\phi)$ and $f = f(X, \Box X)$.

Nevertheless, assuming we modify P_s to include a constant term, or more generally a $l(\phi)$ contribution, and get the GCG simultaneously, would lead to a modification in the Lagrangian of the form $\mathcal{L}_s \to \mathcal{L}_s - l(\phi)$ that however disagrees with the requirement to shift $P_s \to P_s + l(\phi)$. Consequently, there is no chance to include into a GCG a pure constant contribution working out with one single dynamical field, identified by ϕ and X.

A. Double field approach

As a byproduct of our conjecture, we justify the need of introducing a double-field, noncoupled Lagrangian of the form

$$\mathcal{L} = b(\phi)f(X) + Y - V^{\text{eff}}(\psi). \tag{5}$$

Here, it is interesting to focus on each term, emphasizing the role of generalized kinetic energy and potential. Particularly,

(i) ψ represents the second field, whose kinetic energy is $Y \equiv \partial_\sigma\psi\partial^\sigma\psi$, and
(ii) V^{eff} is the second field potential providing the main departures from the pure GCG case. Specifically, we require it to furnish a further vacuum energy

contribution modifying the net GCG EoS and, *de facto*, resolving the conceptual issues prompted above.

Accordingly, the first field is free, while the second is modeled through the inclusion of scalar field potential with vacuum energy.

The first step is therefore to reproduce the GCG-like part of the total EoS. So, we consider [58]

$$f(X) = \left(1 - X^{\frac{1+\alpha}{2\alpha}}\right)^{\frac{1+\alpha}{\alpha}}, \tag{6}$$

and, varying the corresponding action with respect to the metric tensor $g_{\mu\nu}$, we obtain the energy-momentum tensor

$$T_{\mu\nu} = \frac{b(\phi)X^{\frac{1-\alpha}{2\alpha}}}{\left(1 - X^{\frac{1+\alpha}{2\alpha}}\right)^{\frac{1}{1+\alpha}}}\partial_\mu\phi\partial_\nu\phi - 2\partial_\mu\psi\partial_\nu\psi + \mathcal{L}g_{\mu\nu}. \tag{7}$$

In particular, the GCG, as well as many other fluid-based cosmological models, can be put into correspondence with scalar fields or tachyons. Hence, to fulfill the existence of a second fluid exhibiting a vacuum energy contribution, it appears straightforward to write down the corresponding potential by

$$V_{\text{Murnaghan}} = V_0 + V_1(\psi^2 - v^2)^2, \tag{8}$$

that represents the simplest approach to enable a scalar field to transport vacuum energy, once falling into one of the two minima, $\psi = \pm v$. This scenario represents a quartic power-law potential that breaks the symmetry of the system, while falling into $\pm v$.

We can reinterpret this choice of the potential in terms of the so-called *Murnaghan EoS*, corresponding to a GCG plus vacuum energy. Indeed, a direct comparison with the perfect fluid energy-momentum tensor provides

$$\rho = \frac{b(\phi)}{\left(1 - X^{\frac{1+\alpha}{2\alpha}}\right)^{\frac{1}{1+\alpha}}} - 2Y - V_0 - V_1(\psi^2 - v^2)^2, \tag{9a}$$

$$P = -b(\phi)\left(1 - X^{\frac{1+\alpha}{2\alpha}}\right)^{\frac{\alpha}{1+\alpha}} + V_0 + V_1(\psi^2 - v^2)^2, \tag{9b}$$

where the four-velocities for the fields ϕ and ψ are given by $u_\mu = \partial_\mu\phi/\sqrt{X}$ and $v_\mu = \partial_\mu\psi/\sqrt{Y}$, respectively.

It appears evident that, as $\psi \to \pm v$, a vacuum energy contribution remains in both density and pressure, under the form of a nonzero offset, $V_0 > 0$.

For the sake of completeness, every potential of the form

$$V' \to V_{\text{Murnaghan}}G(\psi), \tag{10}$$

with the additional potential $G(\psi)$ fulfilling the condition $G(v) = G(-v) = 1$, can be used to describe the Murnaghan potential that therefore is not unique.

In this work, by virtue of the freedom in choosing $V(\psi)$, we focus on Eq. (8) only in order to require the existence of an effective cosmological constant associated with the second field, ψ.

Hence, choosing the minimum v, once the symmetry is broken as $\phi \to v$ and $Y \to 0$, by introducing a shift of the density $\rho \to \rho - V_0$, Eq. (9) reduce to the EoS

$$P = -\frac{b(\phi)^{1+\alpha}}{\rho^\alpha} + V_0. \tag{11}$$

This, however, has been achieved by working out a shift of the density that is valid only *after the transition induced by the symmetry-breaking potential*. In such a case we are able to freeze-out the kinetic term of ψ, that in general differs from X.

The above finding is manifestly a GCG with an additional constant term, reinterpreted as a cosmological constant, predicted by vacuum energy. Naively, because of the presence of the offset V_0, the model can exhibit regimes in which dark energy arises naturally, leading however to the existence of a matter fluidlike that provides pressure at all stages of the universe evolution.

In the next section, we discuss the physics of this fluid from a macroscopic perspective.

III. MACROSCOPIC INTERPRETATION OF TACHYONIC FLUID WITH BARE COSMOLOGICAL CONSTANT TERM: THE THERMODYNAMIC ACCELERATON

Bearing Eq. (11) in mind, we reinterpret it in terms of the so-called *Murnaghan EoS*, that in standard thermodynamics is constructed with an additive constant contributing to a GCG and resembling the aforementioned approach that uses fields.

Specifically, in solid state physics, the Murnaghan EoS establishes a relationship between the volume V and the pressure P of a given physical system that features the behavior of matter under high pressure. Its thermodynamics reflects that experimentally the more a solid is compressed, the more difficult is to compress it further. This process is related to characteristics such as Poisson coefficient, compressibility, etc. [62], and is extremely similar to what happens in the context of the Anton-Schmidt fluid [63], recently characterized as an extensions of logotropic fluids [64].

Thus, the basic assumption behind the Murnaghan EoS is that the bulk modulus of the incompressibility $K = -V(\partial P/\partial V)_T$ at constant temperature T is a linear function of pressure given by $K = K_0 + K_0'P$. This provides a pressure defined as

$$P = \frac{K_0}{K_0'}\left[\left(\frac{V}{V_0}\right)^{-K_0'} - 1\right], \tag{12}$$

where K' is the first derivative of the bulk modulus with respect to P and the subscript "0" labels the values of each quantity describing the system taken when $P = 0$.

A straightforward application of the above EoS in describing the dynamics of the universe can be obtained by considering $V \propto \rho^{-1}$, where ρ is the density. However, key differences exist between solids and the universe.

(i) For the universe, the condition $P = 0$ occurs at intermediate/early times, when the pressureless matter dominates the dynamics, namely, at a normalization density $\rho_\star$ or at volume $V_0 \propto \rho_\star^{-1}$.
(ii) The universe expands, therefore, the volume $V_0 \propto \rho_\star^{-1}$ is smaller than the volume $V \propto \rho^{-1}$ at pressure onset, implying that $\rho_\star > \rho$.
(iii) By definition $K > 0$, so at $P = 0$ it has to be $K_0 > 0$. Similarly, at the on-set of the cosmic pressure $P < 0$ causing the accelerated expansion of the universe, to keep $K > 0$ requires $K_0' < 0$.

In view of the above considerations, we may perform the substitutions $K_0 \to A_\star$ and $K_0' \to -\alpha$, where $\alpha > 0$ and $A_\star > 0$ are constants, therefore, ending up with

$$P = -\frac{A_\star}{\alpha}\left[\left(\frac{\rho_\star}{\rho}\right)^{\alpha} - 1\right]. \tag{13}$$

Equation (13) describes a Chaplygin-like behavior $P \propto \rho^{-\alpha}$ with an additional constant term, as above noticed.

Remarkably, we can notice that the original scalar field scenario assumes two fluids, identified by ψ and ϕ. However, in the Murnaghan picture we focus on one fluid only that unifies dark energy and dark matter under the same standards. While in the Murnaghan model a further constant contribution arises naturally, in the field representation the constant contribution comes from vacuum energy induced by ψ. Nevertheless, since ψ falls in its minimum, the corresponding dynamics for ψ is frozen. This is analogous to claim that we obtain only one dynamical field, namely ϕ, in analogy to the Murnaghan macroscopic representation of having one fluid only.

Interestingly, the magnitude of the constant term, mimicking the cosmological constant, is already tuned and can be compatible with both observations and Weinberg's no go theorem, see e.g. [65]. We will focus on these points later in the text, discussing the cosmological constant problem in view of our framework.

A. Large-scale dynamics

By solving the continuity equation of a dark fluid with the above pressure,

$$\rho' + 3(P + \rho) = 0, \tag{14}$$

where the prime represents the derivative with respect to $\ln a$ and a is the scale factor, in principle, it is possible to obtain the dark fluid density ρ.

This strategy, however, does not provide any analytical solutions. Thus, to explore the feasibility of our EoS, it would be useful to constrain the model parameters A, α and $\rho_\star$ to obtain approximate but meaningful solutions.

In other words, we will approximate our EoS, Eq. (13), for different epochs, demanding that from each epoch we will bound the free parameters of our model.

B. Mimicking a ΛCDM-like solution

The first behavior is associated with reproducing the ΛCDM scenario from our model. To this aim, we utilise the recent constraints on the GCG from Ref. [66], where quasars x-ray and UV flux measurements, *Pantheon* sample of SNe Ia, compact radio quasars from very-long baseline interferometry, and BAO data have been used. Reference [66] provides $\alpha = 0.03^{+0.17}_{-0.14}$. However, in Eq. (13), $\alpha < 0$ implies $P > 0$ and $\alpha = 0$ implies $|P| \to \infty$; hence, it might be $\alpha \gtrsim 0$. Since the scale factor a is related to the redshift z via $a = (1+z)^{-1}$, if $z \approx 0$ or $a_0 \approx 1$ we may approximate $\rho \approx \rho_c$—where $\rho_c = 3H_0^2/(8\pi G)$ is the universe's critical density, $H(a_0) \equiv H_0$ is the Hubble constant and G is the gravitational constant—to get

$$\rho(z) \approx \rho_c\left(\Omega_{\rm DF} + \frac{P}{\rho_c}\right)a^{-3} - P, \tag{15a}$$

$$P \approx -A_\star \ln\left(\frac{\rho_\star}{\rho_c}\right) < 0, \tag{15b}$$

where $\Omega_{\rm DF} \equiv \rho/\rho_c$ is the dark fluid density parameter.

Remarkably, the above result is degenerate with the ΛCDM paradigm, as we required. In fact, including the contributions of pressureless baryonic matter and radiation, we obtain

$$H(a) = H_0\sqrt{\Omega_{\rm M}a^{-3} + \Omega_{\rm R}a^{-4} + \Omega_\Lambda}, \tag{16}$$

where $\Omega_{\rm B}$, $\Omega_{\rm CDM}$, $\Omega_{\rm R}$, and Ω_Λ are the baryonic matter, the cold dark matter, the radiation, and the cosmological constant Λ density parameters, respectively, and their relations are: $\Omega_{\rm M} \equiv \Omega_{\rm B} + \Omega_{\rm CDM}$, $\Omega_{\rm CDM} \equiv \Omega_{\rm DF} - \Omega_\Lambda$, and $\Omega_\Lambda \equiv -P/\rho_c$, and the flat universe prior provides $\Omega_{\rm M} + \Omega_{\rm R} + \Omega_\Lambda \equiv 1$.

C. Mimicking a logotropiclike solution

If K_0 is constant or very weakly dependent upon P, then $K_0' \approx 0$ and from $K_0 = -V(\partial P/\partial V)_T$, one gets $P = -K_0 \ln(V/V_0)$. Resorting the usual substitutions to adapt the result to cosmological purposes, we get

$$P \approx -A_\star \ln\left(\frac{\rho_\star}{\rho}\right) < 0, \tag{17}$$

which generally holds for any value of ρ and not only when $\rho \approx \rho_c$. This result is remarkable, because it closely

resembles the Anton-Schmidt EoS [46,67,68]

$$P = A_n \left(\frac{\rho}{\rho_\star}\right)^{-n} \ln\left(\frac{\rho}{\rho_\star}\right), \tag{18}$$

with the index $n = 0$, related to the Grüneisen parameter $\gamma_G = -1/6$ [69], and the imposition $A_n \to A_\star$. Strictly speaking, Eq. (18) with the constraint $n = 0$ is referred to as logotropic model [45,46].

From the first law of thermodynamics for adiabatic systems and Eq. (17), the energy density ϵ can be expressed in terms of the total matter density $\rho_M(a)$ as

$$\begin{aligned}\epsilon(a) &= \rho_M(a) + \rho_M(a) \int \frac{P[\rho'_M(a)]}{\rho'_M(a)^2} d\rho'_M(a) \\ &= \rho_M(a) - A_\star \left\{1 + \ln\left[\frac{\rho_M(a)}{\rho_\star}\right]\right\}.\end{aligned} \tag{19}$$

By defining in Eq. (19) the quantities

$$B \equiv [\ln(\rho_\star/\rho_M) - 1]^{-1}, \tag{20a}$$

$$A_\star \equiv B\rho_c\Omega_\Lambda, \tag{20b}$$

and dividing by ρ_c, so that $\rho_M(z)/\rho_c \equiv \Omega_M a^{-3}$, we obtain

$$H(a) = H_0\sqrt{\Omega_M a^{-3} + \Omega_R a^{-4} + \Omega_\Lambda(1 + 3B\ln a)}, \tag{21}$$

where we introduced the contribution of the radiation and, knowing that $\Omega_M \equiv \Omega_B + \Omega_{CDM}$, the flat universe prior provides $\Omega_M + \Omega_R + \Omega_\Lambda \equiv 1$.

In Ref. [70], the density $\rho_\star$, is identified with the Planck density $\rho_P = c^5/(\hbar G^2)$, where c is the speed of light and $\hbar$ is the reduced Planck constant. We refer to this case as GL1 model. In general, $\rho_\star$ may be kept as a model parameter through B. We refer to this second case as GL2 model.

D. Mimicking a generalized Chaplygin gaslike solutions

Another interesting approximation of the Murnaghan EoS, that follows from the assumption of a bulk modulus with $K_0 \ll K'_0 P$, is given by

$$P \approx \frac{K_0}{K'_0}\left(\frac{V}{V_0}\right)^{-K'_0}. \tag{22}$$

By substituting $K_0 \to \alpha A_c \rho_\star$ and $K'_0 \to -\alpha$, we obtain the GCG EoS [56]

$$P = -A_c\rho_\star\left(\frac{\rho_\star}{\rho}\right)^{\alpha}. \tag{23}$$

From Eq. (14) we get

$$\Omega_{DF}(a) = \Omega_{DF}\left[A_s + (1 - A_s)a^{-3(1+\alpha)}\right]^{\frac{1}{1+\alpha}}, \tag{24}$$

with $\Omega_{DF}(a) \equiv \rho(a)/\rho_c$ and $\Omega_{DF} \equiv \rho(a_0)/\rho_c$. From the choices made for the model parameters, we have that

$$A_s \equiv A_c\left[\frac{\rho_\star}{\rho(a_0)}\right]^{1+\alpha}, \tag{25a}$$

$$A_\star \equiv \alpha A_c \rho_\star. \tag{25b}$$

Also, A_s can be written in terms of the effective total matter density Ω_M and α as [66]

$$A_s = 1 - \left(\frac{\Omega_M - \Omega_B}{1 - \Omega_B}\right)^{1+\alpha}. \tag{26}$$

Including baryonic matter and radiation, we get

$$H(a) = H_0\sqrt{\Omega_B a^{-3} + \Omega_R a^{-4} + \Omega_{DF}(a)}, \tag{27}$$

where the flat universe prior gives $\Omega_B + \Omega_R + \Omega_{DF} \equiv 1$.

To focus on which epochs are related to the above approximations, we now intend to constrain our models and fix the bounds over the free parameters. We will thus conclude on how to interpret the model throughout the evolution of the universe.

IV. NUMERICAL CONSTRAINTS

In the concordance model, the total energy density can be decomposed into pressure-less (baryonic and dark) matter and cosmological constant Λ. When the Murnaghan EoS is taken into account, the above decomposition is less trivial because the solution of the continuity equation is not analytic and our dark matter component does not exhibit a vanishing pressure. Among the above analyzed approximated solutions of the Murnaghan EoS, we have seen that in ΛCDM-like and logotropic solutions dark energy and dark matter components are "disentangled," whereas in the GCG solution these components are intertwined.

In view of these considerations, the study of the above approximated solutions can provide constraints for the model parameters of the full numerical solution of the Murnaghan EoS. Therefore, we perform a set of MCMC analyses to fix the cosmological bounds over the different paradigms. We employ the standard low-redshift data surveys: OHD [71], the *Pantheon* catalog of SNe Ia [72], and BAO [73], all referring to the cosmological redshift z, which is easier to measure. The best set of model parameters is set by maximizing the total log-likelihood function

$$\ln\mathcal{L} = \ln\mathcal{L}_O + \ln\mathcal{L}_S + \ln\mathcal{L}_B. \tag{28}$$

Below, we define the contribution of each probe.

A. Hubble rate data log-likelihood

OHD are cosmology-independent estimates of the Hubble rate $H(z) = -(1+z)^{-1}\Delta z/\Delta t$, obtained through spectroscopic measurements of the age difference Δt and redshift difference Δz of couples of passively evolving galaxies that formed at the same time [74]. The corresponding log-likelihood function is then given by

$$\ln \mathcal{L}_{\rm O} = -\frac{1}{2}\sum_{i=1}^{N_{\rm O}} \left\{ \ln\left(2\pi\sigma_{H_i}^2\right) + \left[\frac{H_i - H(z_i)}{\sigma_{H_i}}\right]^2 \right\}, \tag{29}$$

where $N_{\rm O} = 32$ corresponds to the OHD data points [71].

B. SNe Ia log-likelihood

The *Pantheon* dataset of 1048 SNe Ia [72] is equivalently described as a $E(z)^{-1} \equiv H_0/H(z)$ catalog, at $N_{\rm S} = 6$ redshifts, which accurately reproduce the cosmological constraints of the whole SN Ia dataset [75]. The corresponding SN log-likelihood function is given by

$$\ln \mathcal{L}_{\rm S} = -\frac{1}{2}\sum_{i=1}^{N_{\rm S}} [E_i^{-1} - E(z_i)^{-1}]^{\rm T}\mathbf{C}_{\rm S}^{-1}[E_i^{-1} - E(z_i)^{-1}] - \frac{1}{2}\sum_{i=1}^{N_{\rm S}} \ln\left(2\pi|\det \mathbf{C}_{\rm S}|\right), \tag{30}$$

where E_k^{-1} are the measurements from SNe Ia and $\mathbf{C}_{\rm S}$ is the covariance matrix [75].

C. BAO log-likelihood

BAO are the observed peaks in the large scale structure correlation function and enable angular measurements in different redshift slabs that might be correlated or not.

For uncorrelated data points we define

$$\Theta(z) \equiv r_{\rm s}\left[\frac{H(z)}{cz}\right]^{\frac{1}{3}}\left[\frac{(1+z)}{d_{\rm L}(z)}\right]^{\frac{2}{3}}, \tag{31}$$

where, for a flat universe, the luminosity distance is

$$d_{\rm L}(z) = c(1+z)\int_0^z \frac{dz'}{H(z')}, \tag{32}$$

and $r_{\rm s}$ is the comoving sound horizon at the baryon drag redshift, calibrated through the CMB data for a given cosmological model. Hereafter we fix $r_{\rm s} = 147.09$ Mpc [76]. The corresponding log-likelihood is given by

$$\ln \mathcal{L}_{\rm B}^{\rm u} = -\frac{1}{2}\sum_{i=1}^{N_{\rm B}^{\rm u}} \left\{ \ln(2\pi\sigma_{\Theta_i}^2) + \left[\frac{\Theta_i - \Theta(z_i)}{\sigma_{\Theta_i}}\right]^2 \right\}, \tag{33}$$

where the $N_{\rm B}^{\rm u} = 8$ measurements are taken from Ref. [77].

For correlated data, we define

$$\Xi(z) \equiv \frac{H_0 r_{\rm s}}{cz}\frac{\sqrt{\Omega_{\rm m}}}{\Theta(z)}, \tag{34}$$

and write the corresponding log-likelihood

$$\ln \mathcal{L}_{\rm B}^{\rm c} = -\frac{1}{2}\sum_{i=1}^{N_{\rm B}^{\rm c}} [\Xi_i - \Xi(z_i)]^{\rm T}\mathbf{C}_{\rm B}^{-1}[\Xi_i - \Xi(z_i)] - \frac{1}{2}\sum_{i=1}^{N_{\rm B}^{\rm c}} \ln\left(2\pi|\det \mathbf{C}_{\rm B}|\right), \tag{35}$$

where the $N_{\rm B}^{\rm c} = 3$ measurements and the covariance matrix $\mathbf{C}_{\rm B}$ are taken from Ref. [78].

Therefore, the full BAO log-likelihood is given by

$$\ln \mathcal{L}_{\rm B} = \ln \mathcal{L}_{\rm B}^{\rm u} + \ln \mathcal{L}_{\rm B}^{\rm c}. \tag{36}$$

D. Numerical results

Table I and Fig. 1 show, respectively, the contour plots and the best-fit parameters got from ΛCDM, GL1, GL2, and GCG models. We parametrized $H_0 = 100h_0$ and fixed $\Omega_{\rm R} = 9.265 \times 10^{-5}$ and $\Omega_{\rm B} = 0.0493$ [76].

The statistical comparison of the above models is based on the *Aikake information criterion* (AIC) and *Bayesian information criterion* (BIC) [79], respectively,

TABLE I. Best-fit and derived parameters (with $1-\sigma$ errors), and statistical tests of ΛCDM, GL1, GL2, and GCG models. As the Murnagham fluid cannot be integrated analytically, we separately fit each of the above approximations, namely the ΛCDM, GL1, GL2 and GCG scenarios, to constrain the free parameters of our overall model, based on the nonminimal coupling between two scalar fields.

	Best-fit parameters				Derived parameters		Statistical tests		
Model	h_0	$\Omega_{\rm M}$	B	α	$\log(\rho_\star/\rho_c)$	$\log(A_\star/\rho_c)$	$-\ln\mathcal{L}$	AIC (BIC)	Δ
ΛCDM	$0.690^{+0.012}_{-0.011}$	$0.304^{+0.028}_{-0.024}$	⋯	⋯	122.76	$-2.608^{+0.019}_{-0.020}$	65.50	135 (139)	0 (0)
GL1	$0.691^{+0.011}_{-0.011}$	$0.305^{+0.027}_{-0.025}$	⋯	⋯	122.76	$-2.610^{+0.019}_{-0.020}$	65.50	135 (139)	0 (0)
GL2	$0.711^{+0.012}_{-0.013}$	$0.358^{+0.031}_{-0.029}$	$0.319^{+0.042}_{-0.041}$	⋯	$1.35^{+0.09}_{-0.12}$	$-1.135^{+0.038}_{-0.042}$	74.98	156 (162)	21 (23)
GCG	$0.691^{+0.014}_{-0.013}$	$0.307^{+0.035}_{-0.028}$	⋯	$0.03^{+0.22}_{-0.17}$	122.76	$-4.971^{+0.019}_{-0.020}$	65.50	137 (143)	2 (4)

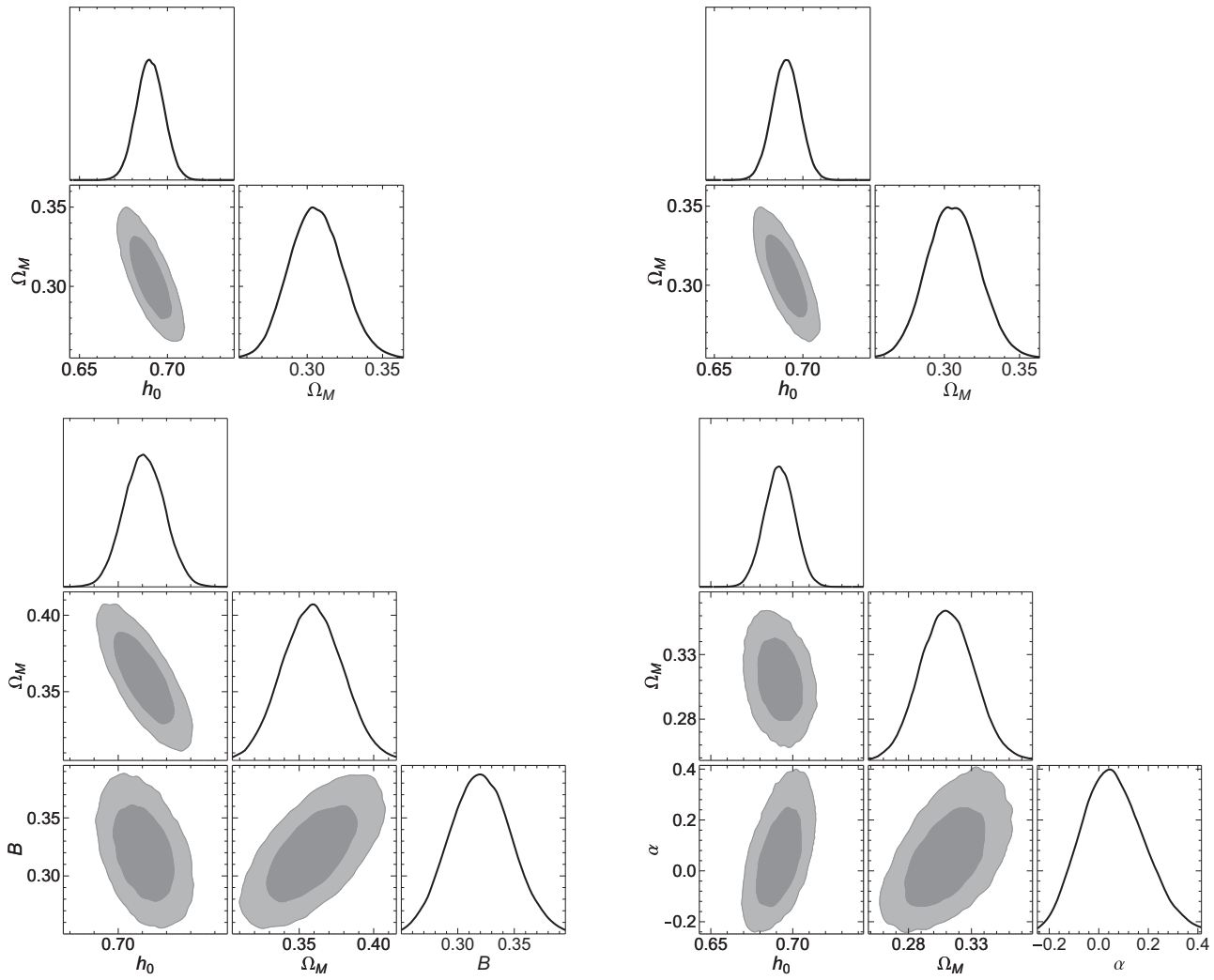

FIG. 1. Contour plots and best-fit parameters (black dots) of ΛCDM (top left), GL1 (top right), GL2 (bottom left), and GCG (bottom right) models. Darker (lighter) areas mark $1-\sigma$ $(2-\sigma)$ confidence regions.

$$\mathrm{AIC} = -2\ln\mathcal{L} + 2p, \tag{37a}$$

$$\mathrm{BIC} = -2\ln\mathcal{L} + p\ln N, \tag{37b}$$

where $\ln\mathcal{L}$ is the maximum of the log-likelihood, p is the number of parameters, and N is the number of data points. The model with the lowest values of the above criteria, labeled with AIC_0 and BIC_0, is referred to as the fiducial (best-suited) model. The comparison between the proposed models and the fiducial one is performed by computing the differences $\Delta = \mathrm{AIC} - \mathrm{AIC}_0$ or $\mathrm{BIC} - \mathrm{BIC}_0$, that provide evidence against the proposed model or, equivalently, in favor of the fiducial one, as follows

(i) $\Delta \in [0,3]$, weak evidence;
(ii) $\Delta \in (3,6]$, mild evidence; and
(iii) $\Delta > 6$, strong evidence.

Looking at the statistical test part of Table I, we can conclude that ΛCDM and GL1 models are equally best-suited to fit the data, the GCG model is weakly/mildly disfavored, whereas the GL2 model is strongly excluded.

V. PHYSICAL INTERPRETATION OF OUR DOUBLE-FIELD MODEL

From the results of the statistical analysis summarized Table I, now we can provide handful constraints on the parameters (α, $\rho_\star$, $A_\star$) of the Murnaghan EoS.

(i) ΛCDM. For this limiting case, we assumed $\alpha \gtrsim 0$. However, we are unable to constrain $\rho_\star$ and $A_\star$ because from Eq. (15) we get only one condition

$$A_\star = \frac{3H_0^2}{8\pi G}\left[\ln\left(\frac{8\pi G\rho_\star}{3H_0^2}\right)\right]^{-1}(1-\Omega_{\mathrm{M}}-\Omega_{\mathrm{R}}). \tag{38}$$

In Table I, to break the above-described degeneracy, we impose $\rho_\star \equiv \rho_{\mathrm{P}}$ and derive $A_\star$.

(ii) GL1 and GL2. Also for these models we assumed $\alpha \gtrsim 0$ but now, from Eq. (20), we are able to set conditions on both $\rho_\star$ and $A_\star$, i.e.,

$$\rho_\star = \frac{3H_0^2\Omega_M}{8\pi G}\exp\left(1+\frac{1}{B}\right), \tag{39a}$$

$$A_\star = \frac{3H_0^2 B}{8\pi G}(1-\Omega_M-\Omega_R). \tag{39b}$$

For the GL1 model, the condition $\rho_\star \equiv \rho_P$ holds, thus in Table I we evaluated only $A_\star$. For the GL2 model, we evaluated both $\rho_\star$ and $A_\star$.

(iii) GCG. In this case α is a model parameter and its best-fit value (see Table I) agrees with the results got in Ref. [66]. On the other hand, like in the ΛCDM case, from Eq. (25) we obtain only one condition

$$A_\star = \alpha\frac{A_s}{\rho_\star^\alpha}\left(\frac{3H_0^2}{8\pi G}\right)^{1+\alpha}(1-\Omega_B-\Omega_R)^{1+\alpha}, \tag{40}$$

that does not allow us to disentangle $\rho_\star$ and $A_\star$ and the expression of A_s is given by Eq. (26).

Now, we can draw some interesting considerations.

(i) At late times, when $a \approx 1$, the Murnaghan EoS in Eq. (13) is approximated by the ΛCDM model for $\rho \approx \rho_c$; the GL1 and GL2 models represent the limiting cases of Eq. (13) for $\rho \neq \rho_c$.

(ii) Looking at Table I, we notice that the GL1 is statistically identical to and degenerates with the ΛCDM model, whereas the model GL2 is strongly excluded. Therefore, since ΛCDM and GL1 models are limiting cases of Eq. (13), we can safely deduce that the condition $\rho_\star \equiv \rho_P$ holds also for the more general Murnaghan EoS.

(iii) At intermediate times $0 \lesssim a \lesssim 1$, once the condition $\rho_\star \equiv \rho_P$ is set-up, the term $(\rho_P/\rho)^\alpha$ dominates and Eq. (13) can be approximated by the GCG model. Since this model is the only one able to constraint the parameter α, we use the corresponding value listed in Table I as a constraint for the Murnaghan EoS.

(iv) Putting together in Eq. (40) the constraint $\rho_\star \equiv \rho_P$ got from ΛCDM and GL1 models and the value of α got from the GCG model, we get the value of $A_\star$ listed in Table I for the GCG case that represents the last constraint for the Murnaghan EoS.

(v) Finally we notice that, at early times, when $a \approx 0$ and $x = \rho_P/\rho \approx 1$, at the lowest order we have $x^\alpha - 1 \approx \ln x^\alpha$, therefore, Eq. (13) becomes the EoS of the GL model in Eq. (17).

In view of the above findings, viable constraints on the parameters of the Murnaghan EoS are

$$\bar{\alpha} = 0.03^{+0.22}_{-0.17}, \tag{41a}$$

$$\bar{\rho}_\star = \rho_P, \tag{41b}$$

$$\bar{A}_\star = (1.07^{+0.05}_{-0.05})\times 10^{-5}\rho_c, \tag{41c}$$

where we indicated with upper bars the parameters, pointing out that those limits are average quantities got from the fits, performed at different times.

The corresponding best-fit cosmological parameters, with associated errors, can be found from the numerical bounds obtained from ΛCDM, GL1 and GCG models, having:

$$\bar{h}_0 = 0.691^{+0.14}_{-0.13}, \tag{42a}$$

$$\bar{\Omega}_M = 0.305^{+0.037}_{-0.026}. \tag{42b}$$

In particular, bearing such intervals in mind, we notice that Fig. 2, top panel, displays the numerical density of the Murnaghan EoS for the parameters $(\bar{\alpha}, \bar{\rho}_\star, \bar{A}_\star)$ listed

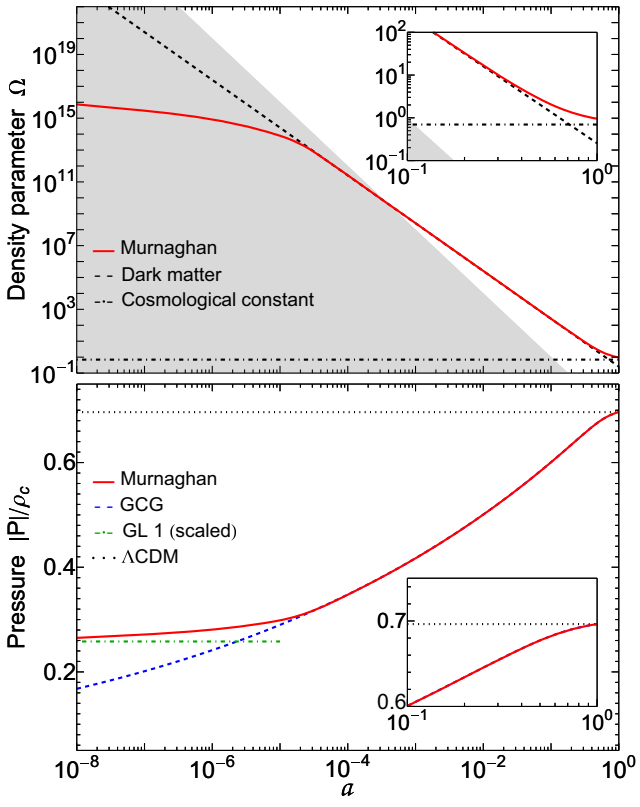

FIG. 2. Top: numerical density from the Murnaghan EoS, compared with dark matter and dark energy behaviors of the ΛCDM case; the shaded area marks the radiation density behavior. Bottom: comparison among the pressures of Murnaghan, GCG, GL1 (rescaled to match the Murnaghan one at $a \to 0$), and ΛCDM. The insets show the behaviors at $0.1 \leq a \leq 1$. The parameter values are taken from Table I.

in Eq. (41) and the cosmological parameters ($\bar{h}_0$, $\bar{\Omega}_{\rm M}$) summarized in Eq. (42). Being a dark fluid numerical solution, it is compared with the dark (matter and energy) sector behaviors obtained with the parameters (h_0, $\Omega_{\rm M}$) taken from the ΛCDM case in Table I.

The comparison of the pressures of Murnaghan, GCG, GL1 (rescaled to match the Murnaghan one at $a \to 0$), and ΛCDM are portrayed in the bottom panel of Fig. 2. The curves, obtained using the values of Table I, show explicitly that the full numerical solution behaves like

(i) ΛCDM and GL1 cases at $a \approx 0$,
(ii) the GCG model at $10^{-5} \lesssim a \lesssim 1$, and
(iii) a scaled GL1 case at $a \lesssim 10^{-5}$.

Hence, we find the physical interpretation below.

(i) At very early times, the model acts as logotropic fluid that reduces to the ΛCDM model. This implies that, in view of structure formation, we do not expect significant departures adopting our model. Phrasing it differently, a similar behavior of our current standard cosmological model is expected even at the level of structure formation.
(ii) At early times, the model appears as a logotropic fluid, being a limiting case of the Anton-Schmidt EoS. This is not in contrast with current knowledge about this epoch, albeit possible comparisons adopting high-distance indicators, such as gamma-ray bursts, would clearly help a lot to check whether the model is well-suited at this stage.
(iii) From intermediate time up to our epoch, the model appears as a Chaplygin gas. Particularly, the model acts as a GCG solution and agrees with late time observations. This behavior can also reconcile the matter-dominated phase with the dark energy-dominated phase, being compatible with our expectations.
(iv) Remarkably, we can wonder whether the Murnaghan EoS can alleviate the h_0 tension. This aspect can be investigated in view of the numerical results that we obtained in Table I. There, apparently the case GL2 can increase the value of h_0 only, although within 1σ the departure from the local value obtained by Riess [80] from Cepheids is only slightly matching. At large redshifts, however, the Murnaghan EoS appears indistinguishable from the ΛCDM paradigm. So, we cannot expect to heal the cosmological tensions on h_0 easily. This can be due to the form of the Murnaghan EoS obtained from a double-scalar field, where the second falls in the minimum. Possibly, assuming a more complicated form of the potential may lead to improvements on the h_0 tension, i.e., generalizing the Murnaghan EoS through more complicated versions.

A. Thermodynamics of matter with pressure

Matter exhibiting pressure behaves as an effective dark energy contribution. Any evolving dark energy components comply with the laws of thermodynamics and might be described as perfect fluids, particularly in the context of background cosmology. Specifically, the role of specific heats in cosmology has been examined in light of observational data [81], showing that dark energy exhibits strange behavior for specific heats, similar to the case of black holes, where the specific heat appears negative [82].

Our EoS mimics dark energy as due to the different thermodynamic stages throughout the universe evolution. This may be prompted easily, emphasizing how it can extend the standard ΛCDM model, by simply working out the adiabatic indices coming from the requirement that heat capacities are constructed in equilibrium thermodynamics for the matter fluid itself, namely assuming they can evolve with time.

As in standard thermodynamics, the heat capacities conform to the relationship between internal energy, enthalpy, and so, in view of the fact that the thermal exchange process is purely adiabatic, implying that the volume scales as $V \propto a^3$, the inferred dark energy contribution exhibits weak interactions with the other constituents, behaving akin to a gaseous fluid source in Einstein's equations.

So, we consider the possibility that the adiabatic index, denoted as γ, can take specific values while excluding regions where it is not allowed to vary. To do so, we resort the definition of internal energy and enthalpy,

$$U = \rho V, \tag{43a}$$

$$h = (\rho + P)V, \tag{43b}$$

respectively, which are positive definite functions of the volume V, the pressure P, and the temperature T. Since all state variables evolve with z, it is natural to assume the simplest hypothesis where U and h are solely functions of T, so that $\rho = \rho(T)$ and $P = P(T)$. Adopting the standard definition $V = V_0 a^3$, which captures the evolution of the universe at early and late times, and the relations $H'/H \equiv (1+q)(1+z)^{-1}$ and $H''/H \equiv (j - q^2)(1+z)^{-2}$, we define

$$C_P = \frac{2V_0}{T'}\frac{(j-1)}{(1+z)^4}H^2, \tag{44a}$$

$$C_V = \frac{3V_0}{T'}\frac{(2q-1)}{(1+z)^4}H^2, \tag{44b}$$

where q is the deceleration parameter and j the jerk parameter, related to the so-called cosmography of the universe [83–87] and the prime here indicates derivative with respect to the redshift, z. Then, combining these relations among them, the adiabatic index γ yields

$$\gamma = \frac{2(j-1)}{3(2q-1)}. \tag{45}$$

The three allowed regimes are: $0 < \gamma < 1$, $\gamma = 1$ and $\gamma > 1$ and so the consequences on the thermodynamics of dark energy are summarized as follows: $C_V, C_P < 0$ in the first case, $C_P = 0$ and $C_V < 0$ in the second case and $C_V, C_P > 0$ in the last case, and furthermore there also exists a region for which[2] $C_P = 0$ and $C_V = 0$, occurring as $q \to 1/2$ and $j \to 1$. Therefore, we have

$$\gamma = \frac{C_P}{C_V} = \frac{(\rho' + P')V + (\rho + P)V'}{\rho' V + \rho V'}, \tag{46}$$

thus, for each epoch the Murnaghan pressure changes accordingly as we list below.

(i) At primordial time:

$$q \simeq 1, \tag{47a}$$

$$j \simeq 3, \tag{47b}$$

$$\gamma = \frac{4}{3}. \tag{47c}$$

Here, the adiabatic index is positive-definite, as a consequence of the jerk parameter [88]. This indicates an effective polytropic fluid that acts as a cosmological constant plus the contribution of matter and radiation. Clearly, the effective value of the cosmological constant involved in our approximation cannot be exactly that of the ΛCDM model, since it differs due to the offset imposed from the beginning into the Murnhagam EoS. Further, a slight variation in time is also expected, differently from the standard cosmological model, albeit leaving unaltered the signs of C_P and C_V.

(ii) At early times: the model appears as a logotropic fluid, but since at early times we are at very high redshift, again conditions (47) are fulfilled. Hence, once again the model resembles the findings of the standard cosmological model even at this stage, implying a suitable thermodynamics as the specific heats are well-defined. Thus, the condition on γ suggests that very slight departures occur and, consequently, weak changes at the level of perturbations are also expected.

(iii) At our time: the model appears as a GCG. Here, the conditions got in Eq. (47) are clearly violated, having

$$q \simeq -0.5, \tag{48a}$$

$$j \geq 1, \tag{48b}$$

$$\gamma < 0. \tag{48c}$$

Here the model works very differently than the previous case, indicating a negative adiabatic index. This thermodynamic instability has been explored in view of dark energy and appears related to the form of the two specific heats. Specifically, $C_P > 0$ and $C_V < 0$, showing that the dark energy fluid behaves very differently than a standard constituent, although the Mayer relation, $C_P - C_V > 0$ is fully preserved, showing that dark energy is approximately described by means of a perfect gas.

In both the latter cases, the model shows that it corresponds to a polytropic fluidlike with effective pressure, rescaled by a constant term, with $\gamma \simeq \alpha$. The model is therefore long-ranging, when a specific heat is negative, exhibiting a behavior that changes significantly as the universe temperature is modified accordingly. The effect of expansion tends to mostly modify the overall form of P, changing consequently the physics associated with the fluid itself. The effects of this behavior are however more evident at intermediate and small redshifts, while at smaller ones the fluid acts as a matterlike component with small pressure. In this respect, it is possible to model the fluid by assuming a double polytrope. Models like this are written as [89]

$$P = P_1 \rho^{\gamma_1} + P_2 \rho^{\gamma_2}, \tag{49}$$

with $P_1, P_2, \gamma_1, \gamma_2$ constants to be defined. The Murnagham fluid appears therefore a limiting case that occurs as $\gamma_1 < 0$ and $\gamma_2 = 0$, identifying P_2 with the constant value of vacuum energy.

For the sake of completeness, there is a further consideration to take into account. The value of vacuum energy, associated to primordial quantum fluctuations, imposed since the very beginning is *fine-tuned* since it cannot be related to the very large values of quantum fields, but rather to the value measured by the Planck satellite [90]. This is related to the cosmological constant problem, namely the inability to cancel out the degrees of freedom related to high-energy scales associated with quantum fluctuations before and after the phase transition, described in the beginning, at the same time [91]. In other words, our model predicts a matterlike component that arose *only after a fine-tuning mechanism of cancellation has occurred to delete the cosmological constant*. Hence, our model *does not* solve the cosmological constant problem by itself, but rather it assumes that it has been resolved somehow during the transition. A possible explanation toward the value of the constant may arise investigating the microphysics of the Murnaghan EoS, i.e., its quantum origin. This is however beyond the purpose of this work and may be subject of further investigations. For additional details about the kind of cancellation mechanisms, expected to erase the cosmological constant, one can refer to Refs. [48,51,54,55,92,93].

[2]In general, this could happen at a redshift $z \gg 1$, under the hypothesis of de-Sitter contribution to dark energy.

VI. IMPACT OF MATTER WITH PRESSURE ON LINEAR PERTURBATIONS

To form structures in the universe requires small initial density perturbations, most likely due to the clustering of matter. In the linear regime, assuming a homogeneous and isotropic universe [94], the evolution of such matter density perturbations can be express by the matter fluid $\delta = \delta\rho_{\rm M}/\rho_{\rm M}$ and it is described by [46]

$$\delta'' + (S\delta)' + \left(2 + \frac{H'}{H} - \frac{T'}{T}\right)(\delta' + S\delta) - TW\delta = 0, \quad (50)$$

with $S = 3(s-w)$, $T = 1+w$, and $W = 3(1+3s)\Omega(a)/2$. The sound speed entering into perturbations is the adiabatic one and its effect is taken into account by

$$s = c_{\rm s}^2 = \left(\frac{\partial P}{\partial a}\right)\left(\frac{\partial \rho_{\rm M}}{\partial a}\right)^{-1}. \quad (51)$$

Defining the matter component density parameter of the perturbed fluid $\Omega(a)$ and the barotropic index w,

$$\Omega(a) = \frac{\rho_{\rm M}(a)}{E(a)^2}, \quad (52a)$$

$$w(a) = -1 - \frac{2}{3}\frac{H'(a)}{H(a)}, \quad (52b)$$

and introducing the logarithmic growth factor $f = (\ln\delta)'$, Eq. (50) becomes [46]

$$f' + \left(2 + f + \frac{H'}{H} - \frac{T'}{T}\right)(f + S) + S' - TW = 0. \quad (53)$$

The general approach to the solution of Eq. (53) consists of the steps below [46].

(1) The clustering component is assumed to be the dark matter, so one can set $w = 0$.
(2) The phenomenological solution $f \approx \Omega_{\rm M}^{\gamma}(a)$ [95], where γ is the so-called growth index, enables to solve a first-order differential equation for γ.
(3) To linearize the above differential equation in γ, the matter component is assumed to be $\Omega_{\rm m} \approx \mathcal{O}(1)$.
(4) A vanishing sound speed is assumed through $s = 0$.

In the following, we take only the above step 1 and proceed with the numerical evaluations for ΛCDM, GL1, GCG, and numerical Murnaghan models. The numerical comparisons of the Hubble rates, the sound speeds, and the logarithmic growth factors of the Murnaghan, GCG, GL1, and ΛCDM models are portrayed in Fig. 3. The parameter values used in the plots of the ΛCDM, GL1 and GCG models are taken from Table I; the parameters for the Murnaghan model are taken from Eqs. (41) and (42).

The evolution of the Hubble parameter in Fig. 3 (top panel) is portrayed as the relative departure with respect to the reference ΛCDM model. For all models the departure within 1% error for $0 \le a \le 1$.

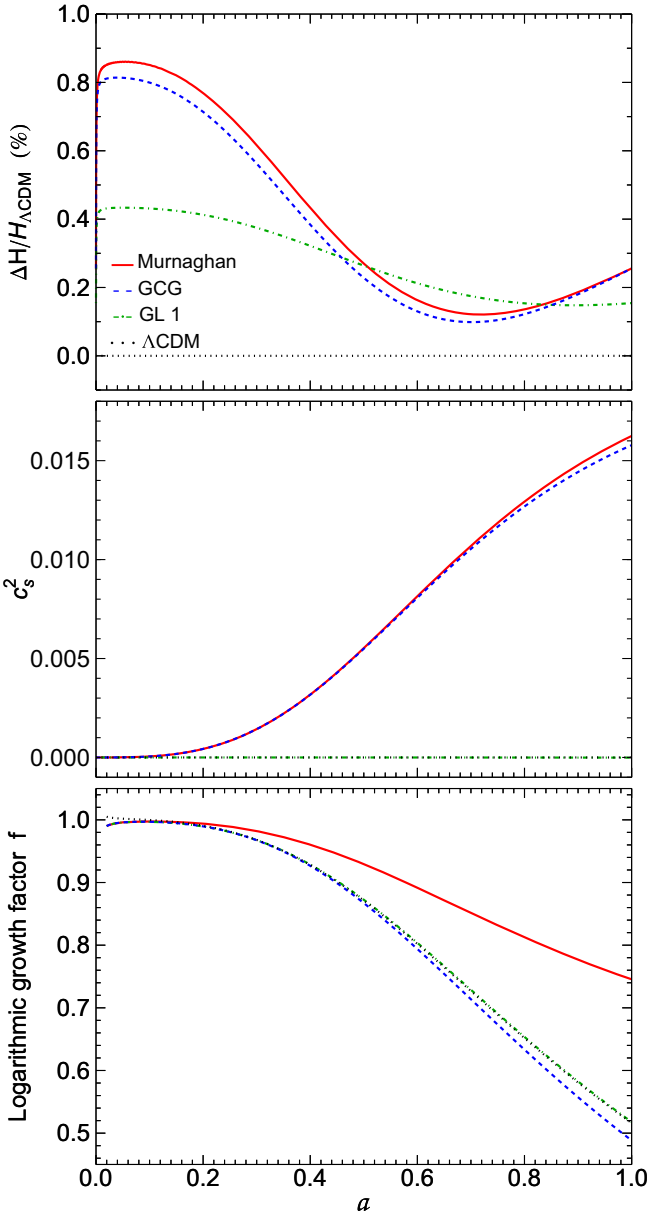

FIG. 3. Numerical comparison among Murnaghan, GCG, GL1, and ΛCDM models. Top: Hubble rate relative differences (with respect to the ΛCDM one). Middle: squared sound speeds. Bottom: logarithmic growth factors. The parameters used in the plots are taken from Table I.

The most interesting quantity for the evolution of perturbations is the adiabatic sound speed, which is shown in Fig. 3 (middle panel). The sound speed determines the stability and the validity of a given model against perturbations.

The evolution of the growth factor f is depicted in the bottom panel of Fig. 3.

The main findings can be easily listed as follows:

(i) All the models derived from the Murnagham EoS have a roughly negligible and positive-defined

sound speeds (identically zero only for the ΛCDM model).

(ii) At very early times, for all models, f flattens and is of the order unity as expected, then it tends to decrease.

(iii) At late times, the small departures of GL1 and GCG models from the ΛCDM one are due to the very small (but non-negligible) values of the sound speeds for these two models.

(iv) On the contrary, for the Murnaghan EoS we have a large deviation from the ΛCDM paradigm, resulting in a more efficient growth of perturbations. This deviation cannot be explained by the sound speed of this model, since it is comparable to the sound speed of the GCG model (see the middle panel of Fig. 3). The main responsible for this effect is the density parameter of the perturbed fluid $\Omega(a)$. Unlike the analytic case of the GCG model, the Murnaghan EoS does not allow us to disentangle the contribution of the dark matter density from the dark fluid density, therefore, $\Omega(a)$ accounts for the total dark fluid density enhancing the growth of perturbations.

VII. FINAL OUTLOOKS AND PERSPECTIVES

We investigated a class of generalized unified dark energy models in which a nonminimal coupling between a tachyonic and scalar fields is introduced. In particular, we demanded that the second field, coupled to the tachyon environment, carries vacuum energy, as predicted by the standard model of particle physics. As a consequence of this recipe, we considered that the second scalar field determines the existence of a vacuum energy term, invoking a corresponding nonremovable offset imposed from a symmetry breaking mechanism.

After the transition, in which the second field appears no longer dynamical, the corresponding EoS appears composed as a sum between a GCG and cosmological constant contribution. We reinterpreted this result in view of the so-called Murnagham EoS, widely-adopted in contexts of solid state physics to characterize those fluids, which under the action of external pressure, tend to act against the pressure itself.

We studied the corresponding dynamics of this model and emphasized the main differences with respect to the GCG. Specifically, since the model is not analytically integrable, we argued how it can reduce to particular cases, such as to the ΛCDM paradigm, to a logotropic fluid and to a Chaplygin gas. To do so, we analyzed each approximation and constrained the corresponding bounds over the free parameters in order to fix them.

Numerical results are taken into account, showing that the model adapts well to cosmic data, as demonstrated by numerical analyses performed by means of MCMC analyses, based on the Metropolis-Hastings algorithm. Using cosmic data, such the OHD, the *Pantheon* SNe Ia and the BAO catalogs, we found limits over the parameters that suggest how the model changes throughout the universe's expansion history.

Precisely, at very early times, we found that the model acts as a logotropic fluid that reduces to the ΛCDM model, while from early to intermediate times, and up to our time, the model appears to described by a GCG. We interpreted our findings in terms of thermodynamics, showing where the model resembles a polytrope and discussing the role of specific heats.

We then determined the evolution of the density contrast in the linear regime. According to our findings about the possible approximations inferred from the Murnagham EoS, we found that in all cases a nonzero sound speed is accounted for. At very early times, the growth factor flattens and is of the order unity as expected, then it tends to decrease. At late times, the small departures of GL1 and GCG models from the ΛCDM one are due to the very small (but non-negligible) values of the sound speeds, while for the Murnaghan EoS we found a large deviation from the ΛCDM paradigm, resulting in a more efficient growth of perturbations. We critically discussed this deviation in view of current observations. We thus concluded that our model appears viable in describing structure formation. Consequences on the h_0 tension are also discussed, in view of possible generalizations of the Murnaghan EoS too.

Consequently, we conclude that our framework appears to be well suited for describing the universe through the action of a single fluid, namely a matterlike fluid with pressure. In other words, we argued that our approach seems to be a suitable candidate to unify dark energy and dark matter under the same standards, applying the nonminimal coupling between two fields, in which at least one of them transports vacuum energy.

Future developments will deal with nonlinear perturbations of the fluid itself. We will also focus on how the thermodynamics of this fluid can justify the negative sign of the pressure. Of particular interest, it will be the discussion on how the Murnaghan EoS can heal the σ_8 tension, as it appears particularly suitable in framing out the cosmological structure formation. Last but not least, we will focus on how to obtain a quantum origin of the Murnaghan EoS, possibly able to find a way out to the cosmological constant problem, in order to obtain more hints toward the nature of unified dark energy models [96].

ACKNOWLEDGMENTS

The work of O. L. is partially financed by the Ministry of Education and Science of the Republic of Kazakhstan, Grant: IRN AP19680128. M. M. acknowledges the support of INFN, iniziativa specifica MoonLIGHT for financial support.

[1] S. Perlmutter *et al.*, Nature (London) **391**, 51 (1998).
[2] A. G. Riess *et al.*, Astron. J. **116**, 1009 (1998).
[3] S. Perlmutter *et al.* (The Supernova Cosmology Project), Astrophys. J. **517**, 565 (1999).
[4] J. L. Tonry *et al.*, Astrophys. J. **594**, 1 (2003).
[5] S. L. Bridle, O. Lahav, J. P. Ostriker, and P. J. Steinhardt, Science **299**, 1532 (2003).
[6] C. L. Bennett *et al.*, Astrophys. J. Suppl. Ser. **148**, 1 (2003).
[7] G. Hinshaw, D. N. Spergel, L. Verde, R. S. Hill, S. S. Meyer, C. Barnes, C. L. Bennett, M. Halpern, N. Jarosik, A. Kogut, E. Komatsu, M. Limon, L. Page, G. S. Tucker, J. L. Weiland, E. Wollack, and E. L. Wright, Astrophys. J. Suppl. Ser. **148**, 135 (2003).
[8] A. Kogut, D. N. Spergel, C. Barnes, C. L. Bennett, M. Halpern, G. Hinshaw, N. Jarosik, M. Limon, S. S. Meyer, L. Page, G. S. Tucker, E. Wollack, and E. L. Wright, Astrophys. J. Suppl. Ser. **148**, 161 (2003).
[9] D. N. Spergel, L. Verde, H. V. Peiris, E. Komatsu, M. R. Nolta, C. L. Bennett, M. Halpern, G. Hinshaw, N. Jarosik, A. Kogut, M. Limon, S. S. Meyer, L. Page, G. S. Tucker, J. L. Weiland, E. Wollack, and E. L. Wright, Astrophys. J. Suppl. Ser. **148**, 175 (2003).
[10] D. J. Eisenstein *et al.*, Astrophys. J. **633**, 560 (2005).
[11] V. Sahni and A. Starobinsky, Int. J. Mod. Phys. D **09**, 373 (2000).
[12] E. J. Copeland, M. Sami, and S. Tsujikawa, Int. J. Mod. Phys. D **15**, 1753 (2006).
[13] S. Tsujikawa, in *Dark Matter and Dark Energy*, Astrophysics and Space Science Library Vol. 370, edited by S. Matarrese, M. Colpi, V. Gorini, and U. Moschella (Springer, Dordrecht, 2011), p. 331.
[14] M. D. Maia, A. J. S. Capistrano, and E. M. Monte, Int. J. Mod. Phys. A **24**, 1545 (2009).
[15] K. Bamba, S. Capozziello, S. Nojiri, and S. D. Odintsov, Astrophys. Space Sci. **342**, 155 (2012).
[16] T. Padmanabhan, Phys. Rep. **380**, 235 (2003).
[17] P. J. Peebles and B. Ratra, Rev. Mod. Phys. **75**, 559 (2003).
[18] S. Capozziello, M. De Laurentis, O. Luongo, and A. Ruggeri, Galaxies **1**, 216 (2013).
[19] E. V. Linder and R. J. Scherrer, Phys. Rev. D **80**, 023008 (2009).
[20] D. Perković and H. Štefančić, Eur. Phys. J. C **80**, 629 (2020).
[21] J. S. Bagla, H. K. Jassal, and T. Padmanabhan, Phys. Rev. D **67**, 063504 (2003).
[22] H.-J. Schmidt, Int. J. Geom. Methods Mod. Phys. **04**, 209 (2007).
[23] S. Nojiri, S. D. Odintsov, and V. K. Oikonomou, Phys. Rep. **692**, 1 (2017).
[24] O. Luongo and H. Quevedo, Found. Phys. **48**, 17 (2018).
[25] K. Bamba, R. Gannouji, M. Kamijo, S. Nojiri, and M. Sami, J. Cosmol. Astropart. Phys. 07 (2013) 017.
[26] C. P. Burgess, *Post-Planck Cosmology: Lecture Notes of the Les Houches Summer School: Volume 100, July 2013* (Oxford Academic, Oxford, 2015).
[27] S. Weinberg, Rev. Mod. Phys. **61**, 1 (1989).
[28] C. Gruber and O. Luongo, Phys. Rev. D **89**, 103506 (2014).
[29] A. Arbey and F. Mahmoudi, Prog. Part. Nucl. Phys. **119**, 103865 (2021).
[30] G. Bertone and T. M. P. Tait, Nature (London) **562**, 51 (2018).
[31] S. Profumo, L. Giani, and O. F. Piattella, Universe **5**, 213 (2019).
[32] C. Pérez de los Heros, Symmetry **12**, 1648 (2020).
[33] S. del Campo, I. Duran, R. Herrera, and D. Pavón, Phys. Rev. D **86**, 083509 (2012).
[34] H. A. Buchdahl, Mon. Not. R. Astron. Soc. **150**, 1 (1970).
[35] L. M. G. Beça and P. P. Avelino, Mon. Not. R. Astron. Soc. **376**, 1169 (2007).
[36] J. Yoo and Y. Watanabe, Int. J. Mod. Phys. D **21**, 1230002 (2012).
[37] P. P. Avelino, L. M. G. Beça, and C. J. A. P. Martins, Phys. Rev. D **77**, 063515 (2008).
[38] M. C. Bento and O. Bertolami, Gen. Relativ. Gravit. **31**, 1461 (1999).
[39] W. Hu and D. J. Eisenstein, Phys. Rev. D **59**, 083509 (1999).
[40] A. Kamenshchik, U. Moschella, and V. Pasquier, Phys. Lett. B **511**, 265 (2001).
[41] N. Bilić, G. B. Tupper, and R. D. Viollier, Phys. Lett. B **535**, 17 (2002).
[42] V. Gorini, A. Kamenshchik, U. Moschella, and V. Pasquier, in *The Tenth Marcel Grossmann Meeting. On Recent Developments in Theoretical and Experimental General Relativity, Gravitation and Relativistic Field Theories* (World Scientific, Singapore, 2006), p. 840.
[43] J. C. Fabris, H. E. S. Velten, C. Ogouyandjou, and J. Tossa, Phys. Lett. B **694**, 289 (2011).
[44] A. Aviles and J. L. Cervantes-Cota, Phys. Rev. D **84**, 089905 (2011).
[45] P.-H. Chavanis, Eur. Phys. J. Plus **130**, 130 (2015).
[46] K. Boshkayev, T. Konysbayev, O. Luongo, M. Muccino, and F. Pace, Phys. Rev. D **104**, 023520 (2021).
[47] O. Luongo and H. Quevedo, Int. J. Mod. Phys. D **23**, 1450012 (2014).
[48] O. Luongo and M. Muccino, Phys. Rev. D **98**, 103520 (2018).
[49] F. D. Murnaghan, Proc. Natl. Acad. Sci. U.S.A. **30**, 244 (1944).
[50] K. Naidoo, M. Jaber, W. A. Hellwing, and M. Bilicki, arXiv:2209.08102.
[51] R. D'Agostino, O. Luongo, and M. Muccino, Classical Quantum Gravity **39**, 195014 (2022).
[52] E. A. Lim, I. Sawicki, and A. Vikman, J. Cosmol. Astropart. Phys. 05 (2010) 012.
[53] P. Jiroušek, K. Shimada, A. Vikman, and M. Yamaguchi, arXiv:2212.14867.
[54] A. Belfiglio, R. Giambò, and O. Luongo, Classical Quantum Gravity **40**, 105004 (2023).
[55] A. Belfiglio, Y. Carloni, and O. Luongo, arXiv:2307.04739.
[56] M. C. Bento, O. Bertolami, and A. A. Sen, Phys. Rev. D **66**, 043507 (2002).
[57] A. Frolov, L. Kofman, and A. Starobinsky, Phys. Lett. B **545**, 8 (2002).
[58] J. C. Fabris, T. C. D. C. Guio, M. H. Daouda, and O. F. Piattella, Gravitation Cosmol. **17**, 259 (2011).
[59] A. Sen, J. High Energy Phys. 04 (2002) 048.
[60] A. Feinstein, Phys. Rev. D **66**, 063511 (2002).
[61] T. Padmanabhan, Phys. Rev. D **66**, 021301 (2002).

[62] A. Aviles, N. Cruz, J. Klapp, and O. Luongo, Gen. Relativ. Gravit. **47**, 63 (2015).
[63] S. Capozziello, R. D'Agostino, and O. Luongo, Phys. Dark Universe **20**, 1 (2018).
[64] H. B. Benaoum, P.-H. Chavanis, O. Luongo, M. Muccino, and H. Quevedo, Astropart. Phys. **151**, 102852 (2023).
[65] M. Nagahama and I. Oda, Phys. Rev. D **97**, 104043 (2018).
[66] J. Zheng, S. Cao, Y. Lian, T. Liu, Y. Liu, and Z.-H. Zhu, Eur. Phys. J. C **82**, 582 (2022).
[67] H. Anton and P. Schmidt, Intermetallics **5**, 449 (1997).
[68] S. Capozziello, R. D'Agostino, R. Giambò, and O. Luongo, Phys. Rev. D **99**, 023532 (2019).
[69] E. Gruneisen, Ann. Phys. (Berlin) **344**, 257 (1912).
[70] P.-H. Chavanis, Phys. Lett. B **758**, 59 (2016).
[71] M. Moresco *et al.*, Living Rev. Relativity **25**, 6 (2022).
[72] D. M. Scolnic *et al.*, Astrophys. J. **859**, 101 (2018).
[73] A. Cuceu, J. Farr, P. Lemos, and A. Font-Ribera, J. Cosmol. Astropart. Phys. 10 (2019) 044.
[74] R. Jimenez and A. Loeb, Astrophys. J. **573**, 37 (2002).
[75] A. G. Riess *et al.*, Astrophys. J. **853**, 126 (2018).
[76] Planck Collaboration, Astron. Astrophys. **641**, A6 (2020).
[77] O. Luongo and M. Muccino, Mon. Not. R. Astron. Soc. **503**, 4581 (2021).
[78] C. Blake *et al.*, Mon. Not. R. Astron. Soc. **418**, 1707 (2011).
[79] A. R. Liddle, Mon. Not. R. Astron. Soc. **377**, L74 (2007).
[80] E. Di Valentino *et al.*, Astropart. Phys. **131**, 102605 (2021).
[81] O. Luongo and H. Quevedo, Gen. Relativ. Gravit. **46**, 1649 (2014).
[82] S. Bhattacharya and S. Shankaranarayanan, Classical Quantum Gravity **34**, 075005 (2017).
[83] O. Luongo, Mod. Phys. Lett. A **26**, 1459 (2011).
[84] A. Aviles, A. Bravetti, S. Capozziello, and O. Luongo, Phys. Rev. D **90**, 043531 (2014).
[85] P. K. S. Dunsby and O. Luongo, Int. J. Geom. Methods Mod. Phys. **13**, 1630002 (2016).
[86] A. Aviles, C. Gruber, O. Luongo, and H. Quevedo, Phys. Rev. D **86**, 123516 (2012).
[87] A. Aviles, J. Klapp, and O. Luongo, Phys. Dark Universe **17**, 25 (2017).
[88] O. Luongo, Mod. Phys. Lett. A **28**, 1350080 (2013).
[89] P. K. S. Dunsby, O. Luongo, and L. Reverberi, Phys. Rev. D **94**, 083525 (2016).
[90] P. Collaboration, N. Aghanim, Y. Akrami, M. Ashdown, J. Aumont, C. Baccigalupi, M. Ballardini, A. Banday, R. Barreiro, N. Bartolo *et al.*, Astron. Astrophys. **641**, A6 (2020).
[91] J. Martin, C. R. Phys. **13**, 566 (2012).
[92] S. Appleby and R. C. Bernardo, J. Cosmol. Astropart. Phys. 12 (2023) 003.
[93] E. V. Linder and S. Appleby, J. Cosmol. Astropart. Phys. 03 (2021) 074.
[94] S. Weinberg, *Gravitation and Cosmology: Principles and Applications of the General Theory of Relativity* (John Wiley and Sons, New York, 1972).
[95] B. C. Paul and P. Thakur, J. Cosmol. Astropart. Phys. 11 (2013) 052.
[96] S. D. Odintsov, V. K. Oikonomou, I. Giannakoudi, F. P. Fronimos, and E. C. Lymperiadou, Symmetry **15**, 1701 (2023).